

Charge-Tunable Optical Properties in Colloidal Semiconductor Nanocrystals

Moonsub Shim,* Congjun Wang, and Philippe Guyot-Sionnest*

James Franck Institute, University of Chicago, Chicago, Illinois 60637

Received: September 29, 2000; In Final Form: November 21, 2000

The optical properties of colloidal semiconductor nanocrystals are found to be extremely sensitive to excess electrons. Electrons in the lowest quantum-confined state of the conduction band of CdSe and (CdSe)ZnS nanocrystals quench photoluminescence by several orders of magnitude, at the same time, leading to a strong, mid-infrared intraband absorption and bleaching of the interband exciton transitions. Surface electrons are also efficient in quenching photoluminescence, but a passivating layer of wider band gap ZnS can reduce their influence. The results suggest that single-electron switching of photoluminescence may be feasible with improved core/shell structures of semiconductor nanocrystals.

Introduction

Recent advances in nanometer-scale semiconductors have provided materials with many novel properties.^{1,2} Device applications such as light-emitting diodes³ and photovoltaic cells⁴ have already been realized. Semiconductor nanocrystals prepared as colloids are a particularly interesting and important class of nanometer-scale materials especially due to the versatility with which they can be manipulated.⁵ Depending on the capping molecules, these nanocrystals can be dispersed in a variety of solvents including those that are suitable for biological environment.^{6,7} They can be manipulated into two- or three-dimensional superlattices.^{8,9} Colloidal semiconductor nanocrystals are exceptionally well suited for studying photophysics and interactions in zero-dimensional materials, and there has been much progress in the control of size distribution,^{5,10} shape,¹¹ and fluorescence efficiency^{12–15} of nanocrystals of various semiconductors.

Recently, the effect of charges has received increased attention:

(i) Photoluminescence (PL) wandering of single nanocrystals^{16,17} has been interpreted as resulting from the motion of surface charges and the associated Stark effect.¹⁷

(ii) Fluorescence intermittency (or blinking), again in single nanocrystals, has been proposed to arise from an Auger recombination process involving the remaining carrier, either an electron or a hole, after a single charge photoionization event.^{18–20} Intraband spectroscopy²¹ has indeed shown that electron-mediated Auger recombination occurs at a much faster rate than radiative recombination.^{22,23}

(iii) An asymmetric surface charge distribution may also explain the large permanent dipole moments observed in wurtzite as well as zinc-blend neutral nanocrystals.²⁴

(iv) Positively charged nanocrystals have been observed when adsorbed on gold substrates.²⁵

(v) Charging energies between 0.1 and 0.2 eV have been measured from solution conductivity²⁴ as well as by scanning tunneling spectroscopy on single nanocrystals²⁶ in agreement with theoretical expectations.²⁷

Therefore, charges are expected to be present and to have strong influence in the optical properties. However, there have been no studies of the optical properties upon charging. In particular, understanding the effects of charges on the photoluminescence may be relevant when semiconductor nanocrystals are utilized as luminescent labels in polar media. It may also help in elucidating the mechanism for blinking observed in single-nanocrystal fluorescence. Controlling the number of charges may lead to a possibility of fine-tuning and improving the optical properties of semiconductor nanocrystals. We present PL, UV/vis, and infrared studies of *n*-type and negatively charged colloidal semiconductor nanocrystals prepared by electron injection from a reducing species.²⁸

Experimental Section

Synthesis of CdSe and (CdSe)ZnS Nanocrystals. Colloidal nanocrystals of CdSe are made in a similar manner as described in ref 5. (CdSe)ZnS (core)shell nanocrystals are prepared by the methods described in refs 12 and 13.

Preparation of *n*-Type Nanocrystals. The *n*-type nanocrystals are made as described in ref 28. Briefly, to 0.3 mL of dried and deaerated solution of nanocrystals with a small amount of TOPO (<5 mg/mL) in 2,2,4,4,6,8,8-heptamethylnonane is added ~10–50 μ L of 1.2 M sodium biphenyl. The concentrations of nanocrystals are such that the optical density of the sample at the first exciton maximum is between 0.5 and 1.5 for 200 μ m path length. Samples are prepared and filled into a cell in the absence of oxygen and closed in a N₂-filled glovebox. The cell is made of one CaF₂ window and a sapphire window separated by a Teflon spacer and is capped with Teflon stopcocks. For all experiments discussed here, samples are brought out of the glovebox after capping and left standing in ambient conditions during and between measurements. While the cell is solvent-tight, long exposure to air causes oxidation of the samples.

Optical Measurements. PL spectra are measured with Perkin-Elmer LS 50 B luminescence spectrometer. IR spectra are obtained with Nicolet Magna 560 FTIR spectrometer. UV/vis spectra are obtained with HP 8453 photodiode array spectrometer. All measurements are carried out at room temperature. No photodegradation has been observed under ambient lighting or spectrometer light sources.

* To whom correspondence should be addressed. E-mail: M.S., mshim@uchicago.edu; P.G.-S., pgs@uchicago.edu.

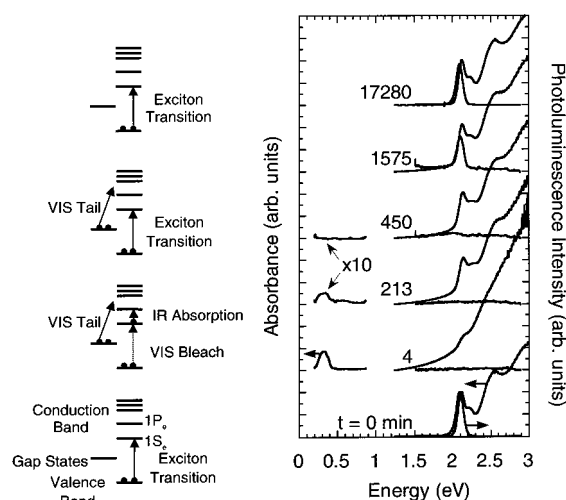


Figure 1. UV/vis and IR absorption and PL spectra of CdSe nanocrystals at different times after exposure to sodium biphenyl and schematic representations of the corresponding electron occupation. The spectrum corresponding to $t = 0$ min is before exposure to sodium biphenyl. Upon electron transfer from biphenyl radical anions, n -type nanocrystals exhibit strong mid-IR absorption along with a concurrent bleach of the exciton transitions in the visible. A complete quenching of PL is also observed. Note that middle 4 PL spectra are scaled 100 times for clarity.

Results and Discussion

After electrons are injected from the strongly reducing sodium biphenyl, a slow oxidation proceeds due to the ambient surrounding. What controls the oxidation rate and ultimately the long-term stability of the n -type material is a subject that we are currently investigating but do not fully understand yet. The oxidation rate is quenched at low temperatures and strongly increased in the presence of air or water. It also depends on the solvent, presumably due to its dryness and polarity. The kinetics of oxidation is sensitive to the material, faster for CdSe than ZnO, and generally faster for smaller sizes, in accord with their relative redox potentials.²⁸ Some decomposition can also occur as evidenced by a small blue-shift in the visible absorption peak observed in both CdSe and (CdSe)/ZnS nanocrystals.

The evolution of the nanocrystal electron occupation after the electron injection is depicted on the left-hand side of Figure 1. A general evolution of the optical properties can be described as follows:

(1) In the highest observed charged state, electrons occupy the lowest conduction band state, $1S_e$, as evidenced by the strong, size-tunable IR absorption from $1S_e$ to $1P_e$. The corresponding population of the $1S_e$ state can be estimated from the observed bleach of the lowest exciton transition since a complete bleach of the first exciton arises for a two-electron occupation of $1S_e$. Similar bleach of the first exciton upon photoexcitation has previously been observed by microsecond to femtosecond transient absorption.^{29–32} Here the bleach is observable over hours to days.

In addition to the quantum-confined states, there may be gap states. In these nanometer-size semiconductors, the most likely gap states are the surface states^{33–35} rather than interior defects. The occupation of these surface states can lead to broadening and shifting of the optical spectrum via the Stark effect.¹⁷ Furthermore, transitions from the surface states and the $1S_e$ state (to a lesser extent for the latter since most of their oscillator strength is in the $1S_e-1P_e$ transition) to higher quantum-confined excited states may lead to a broad optical absorption. Photolu-

minescence may be quenched by two distinct mechanisms: three-body Auger process involving electrons in the $1S_e$ state; hole trapping by the electron-rich surface followed by a nonradiative recombination.

(2) As oxidation proceeds, leaving electrons only in the surface states, the IR absorption and the bleach of the lowest exciton disappear. The shifts and broadening of the visible spectrum due to the Stark effect as well as the broad absorption from occupied surface states may remain. Again, PL may be quenched either by an Auger process or by hole trapping involving the occupied surface states.

Both CdSe and (CdSe)/ZnS nanocrystals follow this two-step process. Differences arise from the better passivation of ZnS on CdSe resulting in smaller influence of surface trapped electrons.

CdSe Nanocrystals. The visible and IR absorption and the PL spectra of TOPO-capped CdSe nanocrystals before addition of sodium biphenyl are shown at the bottom of Figure 1. After addition of sodium biphenyl, a complete quenching of the band-edge luminescence is observed while there is a strong IR absorption ($t = 4$ min). The quenching remains after the IR absorption has completely disappeared ($t = 450$ min). The PL begins to recover well after ($t = 1575$ min) the complete decay of the IR absorption. Note that the middle four PL spectra are scaled 100 times that of the initial spectra for clarity.

To quantify the bleach of the exciton peaks and to separate out the contributions from broadening and Stark shifts as well as from the absorption tail, the spectra are fitted to a sum of Gaussians for the initial features and a rising power for the band-edge tail.³⁶ Figure 2B,C shows the results of this fitting procedure. Note that the biphenyl radical anions can be considered to be instantaneously oxidized in the time scale of the current measurements since the absorption feature of biphenyl radical anion at ~ 1.9 eV is not seen when they are exposed to the solution of nanocrystals. Therefore, no contribution of biphenyl radical anion to the visible spectra of nanocrystals is present.

Comparison of Figure 2A,B indicates that all three exciton peaks are bleached upon electron occupation of the $1S_e$ state of the conduction band. The first two exciton peaks have been assigned to transitions involving $1S_e$, and they are expected to have large and identical bleach.³⁷ The third peak overlaps with transitions involving both $1S_e$ and $1P_e$ states, and the bleach likely arises from the $1S_e$ contribution.

The average number of electrons occupying $1S_e$ state is estimated from the decrease in the area of the Gaussian fit corresponding to the first exciton transition normalized to account for a 2-electron maximum. For the sample in Figure 2B, the bleach in the first exciton transition gives an average of 1.4 ± 0.2 electrons in the $1S_e$ state immediately after exposure to sodium biphenyl. As shown in Figure 3, the visible bleach decay follows the IR absorption closely. This is expected since both the bleach and the IR absorption arise from electron occupation of $1S_e$ state. However, there is a residual 15% bleach which may be attributed to surface negative charges perturbing the electron and the hole states, possibly by mixing $1S_e$ and $1P_e$ states.

The broad band-edge tail is taken as a measure of the number of electrons in surface states because its intensity diminishes only after the $1S_e$ state is empty. When the PL recovers to half its initial value, about 5% of the band-edge tail remains. Assuming that one surface electron can completely quench the fluorescence, this point corresponds to about 0.5 electrons/

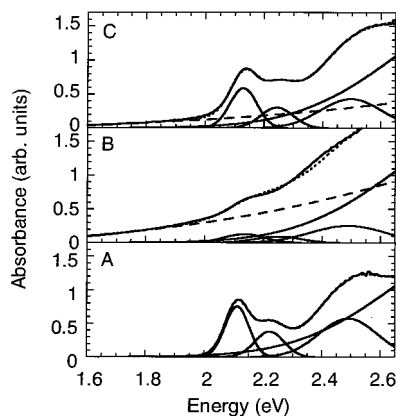


Figure 2. Demonstration of fitting procedure to quantify the changes in the visible absorption spectra of CdSe nanocrystals. The absorption spectrum before exposure to sodium biphenyl (A) is fitted to a sum of four Gaussians (shown below the spectrum). The absorption spectra after exposure to sodium biphenyl (B) is 4 min and (C) is 450 min after) are also fitted to a sum of Gaussians and a rising power (dashed line) for the tail. The dotted lines are the fits and the Gaussians shown below each spectrum are reconstructed from the parameters of the fit. See ref 36 for details of the fitting procedure.

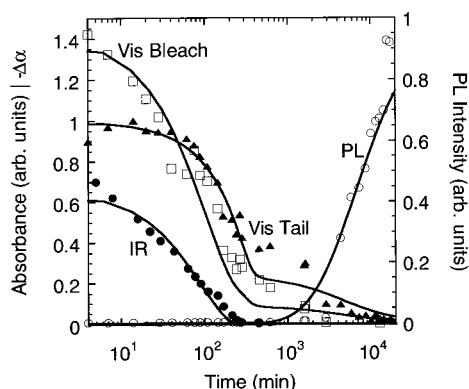


Figure 3. Time evolution of visible and IR properties of CdSe nanocrystals after electron transfer. IR absorption (filled circles) is the maximum absorption normalized for comparison. The visible bleach (open squares) is the difference in the area of the fitted Gaussian (see ref 36) for the first exciton transition then normalized for a 2-electron maximum. The visible absorption tail (filled triangles) is obtained from the coefficient of the rising power in the fit then normalized for comparison. Photoluminescence (open circles) is normalized with respect to initial PL intensity. The lines are from a simple model described in the text.

nanocrystal. Assuming further that the absorbance of the band-edge tail is linearly proportional to the number of electrons in surface states, we estimate that there are about 8–10 electrons in the surface states.

The logarithmic time dependence of the evolution of the optical properties suggests a titration process. A titration model³⁸ is then used to qualitatively fit the results in Figure 3 (solid lines). With an introduction of an oxidant (possibly water) at a constant rate, the chemical equilibrium between nanocrystals of different number of charges and the oxidant is solved. In this model, the nanocrystals can have at most 2 electrons in the $1S_e$ state and 8 surface electrons. The energies of the surface states are determined by a visual best fit to the data. The $1S_e$ state is at 0 eV, and there are a 4-electron state at -0.02 eV, a 2-electron state at -0.16 eV, and a 2-electron state at -0.3 eV. The oxidant is at -0.24 eV (if a charging energy identical for each electrons is introduced, the same equilibrium is obtained with an oxidant redox potential increased by the charging

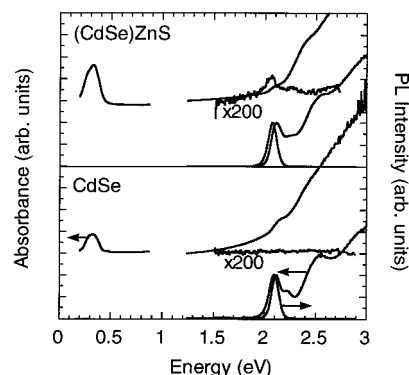


Figure 4. Comparison of the optical changes in ZnS-coated and uncoated CdSe nanocrystals upon electron transfer. Lower spectra in each half of the figure are before exposure to sodium biphenyl. Top spectra of each half are immediately (2–4 min) after.

energy). In this titration model, the PL is taken to be proportional to the concentration of nanocrystals with no charges. The bleach is proportional to the electron occupation of the $1S_e$ state plus a 2% contribution/surface charge. The IR absorption is proportional to the electron occupation of the $1S_e$ state divided by 2 so that it does not overlap with the bleach in the figure. The band-edge tail is proportional to the surface charges normalized to 1 at early times.

The small shift of the surface states with respect to $1S_e$ suggests that they have mostly Cd character. It is unclear at this stage whether the traps are intrinsic to the nanocrystals or are instead generated by the strongly reducing environments, removing some of the ligands for example. We also note that such shallow Cd surface states, even if present in the neutral nanocrystals, may not be optically observed. Indeed, hole states at the top of the valence band and Cd shallow surface states should have a very small overlap. Most of the transitions to the shallow surface states should involve hole states deeper in the valence band, thus being masked by the stronger exciton transitions. It should also be noted that the titration model is only meant to be a guideline in describing the changes in the optical properties of reduced nanocrystals and not to be taken as a definitively quantitative analysis of the observations.

(CdSe)ZnS (Core)shell Nanocrystals. Figure 4 compares the changes in the optical properties of ZnS coated and uncoated CdSe nanocrystals of similar core size as they are made *n*-type. Notice that while there is approximately the same amount of visible bleach of the first two exciton peaks, (CdSe)ZnS exhibits much less of the band-edge tail. Analysis of the first exciton bleach gives about 1.9 electrons initially in the $1S_e$ state. The recovery of the visible bleach follows the IR absorption decay closely (Figure 5). When PL recovers to 50%, there is about 30% of the band-edge tail remaining, which is indicative of 2–4 electrons in surface states, significantly less than that of uncoated CdSe. This observation that (CdSe)ZnS has, on average, less electron traps than CdSe is consistent with the improved luminescence afforded by the ZnS coating¹² and with the expectation that the Zn-derived surface states should be higher in energy than the core conduction band minimum.

For *n*-type (CdSe)ZnS, although the $1S_e$ state is nearly fully populated, the quantum yield is about 10^{-3} relative to the neutral state. This small but nonzero quantum yield is consistent with an Auger rate of ~ 100 ps (in the 2 electron–hole pair limit for ~ 5 nm diameter CdSe nanocrystals^{22,23}) and a fluorescence lifetime of 100 ns. It is also significant that the PL recovery begins when there is about half of the initial IR absorption or ~ 1 electron in the $1S_e$ state. In fact, the PL from nanocrystals

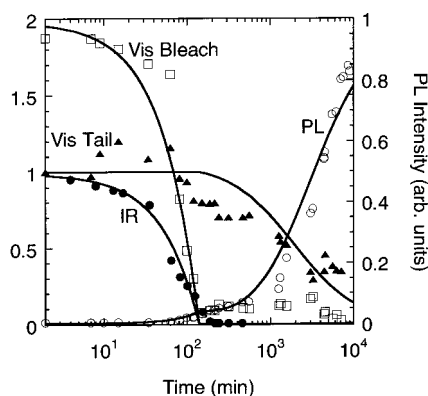


Figure 5. Time evolution of visible and IR properties of (CdSe)ZnS (core)shell nanocrystals after electron transfer from sodium biphenyl. The same description as Figure 3 caption applies.

with remaining surface charges is about 4% of the original PL and at least 2 orders of magnitude larger than in uncoated CdSe nanocrystals with surface charges. This behavior can be understood from the wider band gap ZnS reducing the coupling between surface states and core states leading to a weaker PL quenching. Alternatively, the 4% PL level can be due to 4% of the nanocrystals having no surface band gap states to accommodate excess electrons. In either case, the additional quenching of the PL upon occupation of the $1S_e$ state is a strong support for electron-mediated Auger recombination since it is unlikely to be due to the $1S_e$ electrons increasing the hole trapping rate.

The lines shown in Figure 5 are the results of identical equilibrium considerations as described in the previous subsection except that only a 2-electron deep trap is considered ($1S_e$ state at 0 eV, a 2-electron trap state at -0.3 eV, and the oxidant redox potential at -0.24 eV). We neglect the contribution of surface charges to the visible bleach, and a 4% PL relative efficiency for nanocrystals with only surface charges must be included to account for the PL recovery.

Photoluminescence Properties. A comparison of the results of CdSe and (CdSe)ZnS nanocrystals strongly suggests that the electron-mediated Auger recombination process is dominant when the electron is in $1S_e$. The mechanism by which the excess surface electrons quench the PL could, however, be a combination of both Auger and hole-trap mechanisms. The hole-trap mechanism requires a nonradiative transition from the valence band to the electron surface states. These are derived from the Cd surface atoms, and they should be about 2 eV above the valence band. The trapping rate may then be too slow. On the other hand, the strong absorption tail at the band edge, if arising truly from transitions between the surface electrons and the interior states, implies that an Auger process should be efficient.

It is interesting to note that water-soluble nanocrystals (e.g. silica-coated (CdSe)CdS⁶ and mercaptoalkanoic acid capped (CdSe)ZnS⁷) exhibit reduced quantum yields relative to their TOPO-capped counterparts in nonpolar organic solvents. Due to the lower charging energy in a polar medium, these nanocrystals are more prone to surface charges which may explain the reduced fluorescence efficiencies.

Conclusions

We have shown that electron transfer causes dramatic changes in the optical properties of colloidal semiconductor nanocrystals. In both CdSe and (CdSe)ZnS nanocrystals, there is a strong IR absorption corresponding to the $1S_e-1P_e$ transition when they are made *n*-type. Concurrent bleach of the exciton transitions

accompanies the IR absorption. The photoluminescence is strongly quenched in these negatively charged nanocrystals. We have found that both surface charges and delocalized electrons lead to strong quenching, the latter via an Auger process. These observations suggest that one simple way of controlling the optical properties is to control the number of electrons or the Fermi level in semiconductor nanocrystals. Improved surface passivation or electron injection conditions may lead to the possibility that the fluorescence of semiconductor nanocrystals can be fully quenched by injection of a single electron.

Acknowledgment. This work was funded by the National Science Foundation under Grant No. DMR-9731642. We made use of the MRSEC Shared Facilities supported by the National Science Foundation under Grant No. DMR-9400379.

References and Notes

- (1) Nirmal, M.; Brus, L. E. *Acc. Chem. Res.* **1999**, *32*, 407.
- (2) Alivisatos, A. P. *Science* **1996**, *271*, 933.
- (3) Colvin, V. L.; Schlamp, M. C.; Alivisatos, A. P. *Nature* **1994**, *370*, 354.
- (4) Dabbousi, B. O.; Bawendi, M. G.; Onitsuka, O.; Rubner, M. F. *Appl. Phys. Lett.* **1995**, *66*, 1316.
- (5) O'Regan, B.; Grätzel, M. *Nature* **1991**, *353*, 737.
- (6) Murray, C. B.; Norris, D. J.; Bawendi, M. G. *J. Am. Chem. Soc.* **1993**, *115*, 8706.
- (7) Bruchez, M., Jr.; et al. *Science* **1998**, *281*, 2013.
- (8) Chan, W. C.; Nie, S. *Science* **1998**, *281*, 2016.
- (9) Murray, C. M.; Kagan, C. R.; Bawendi, M. G. *Science* **1995**, *270*, 1335.
- (10) Collier, C. P.; Vossmeier, T.; Heath, J. R. *Annu. Rev. Phys. Chem.* **1998**, *43*, 371.
- (11) Micic, O. I.; et al. *J. Phys. Chem.* **1994**, *98*, 4966.
- (12) Peng, X.; et al. *Nature* **2000**, *404*, 59.
- (13) Hines, M. A.; Guyot-Sionnest, P. *J. Phys. Chem.* **1996**, *100*, 468.
- (14) Dabbousi, B. O.; Rodriguez-Viejo, J.; Mikulec, F. V.; Heine, J. R.; Mattoussi, H.; Ober, R.; Jensen, K. F.; Bawendi, M. G. *J. Phys. Chem. B* **1997**, *101*, 9463.
- (15) Peng, X.; et al. *J. Am. Chem. Soc.* **1997**, *119*, 7019.
- (16) Cao, Y.; Banin, U. *Angew. Chem., Int. Ed. Engl.* **1999**, *38*, 3692.
- (17) Blanton, S. A.; Hines, M. A.; Guyot-Sionnest, P. *Appl. Phys. Lett.* **1996**, *69*, 3905.
- (18) Empedocles, S.; Bawendi, M. G. *J. Phys. Chem.* **1999**, *103*, 1826.
- (19) Nirmal, M.; et al. *Nature* **1996**, *383*, 802.
- (20) Banin, U.; Bruchwz, M.; Alivisatos, A. P.; Ha, T.; Chemla, D. S. *J. Chem. Phys.* **1999**, *110*, 1195.
- (21) Kuno, M.; Fromm, D. P.; Hamann, H. F.; Gallagher, A.; Nesbitt, D. J. *J. Chem. Phys.* **2000**, *112*, 3117.
- (22) Guyot-Sionnest, P.; Hines, M. A. *Appl. Phys. Lett.* **1998**, *72*, 686.
- (23) Guyot-Sionnest, P.; Shim, M. S.; Matrangola, C.; Hines, M. A. *Phys. Rev. B* **1999**, *60*, R2181.
- (24) Klimov, V. I.; et al. *Science* **2000**, *287*, 1011.
- (25) Shim, M.; Guyot-Sionnest, P. *J. Chem. Phys.* **1999**, *111*, 6955.
- (26) Krauss, T. D.; Brus, L. E. *Phys. Rev. Lett.* **1999**, *83*, 4840.
- (27) Banin, U.; Cao, Y.; Katz, D.; Millo, O. *Nature* **1999**, *400*, 542.
- (28) Franceschetti, A.; Zunger, A. *Appl. Phys. Lett.* **2000**, *76*, 1731.
- (29) Shim, M.; Guyot-Sionnest, P. *Nature* **2000**, *407*, 981.
- (30) Dimitrijevic, N. M.; Kamat, P. V. *J. Phys. Chem.* **1987**, *91*, 2096.
- (31) Woggon, U.; Giessen, H.; Fluegel, B.; Peyghambarian, N. *Phys. Rev. B* **1996**, *54*, 17681.
- (32) Burda, C.; Link, S.; Green, T. C.; El-Sayed, M. A. *J. Phys. Chem. B* **1999**, *103*, 10775.
- (33) Klimov, V. I. *J. Phys. Chem. B* **2000**, *104*, 6112.
- (34) Serce, P.; Efros, A. L.; Rosen, M. *Phys. Rev. Lett.* **1999**, *83*, 2394.
- (35) Fu, H.; Zunger, A. *Phys. Rev. B* **1997**, *56*, 1496.
- (36) Pokrant, S.; Whaley, K. B. *Eur. Phys. J. D* **1999**, *6*, 255.
- (37) The UV/vis absorption spectrum of nanocrystals before exposure to sodium biphenyl is fitted to a sum of four Gaussians as shown in Figure 3A. The fourth Gaussian at the highest energy (dashed line in Figure 3A) is to take the UV rise in the absorption features into account. Using the parameters of this fit, the amplitude, the position, and the width of this fourth Gaussian is held fixed and the first three are allowed to vary in magnitude, position, and width to account for the bleach, Stark shift, and broadening in the UV/vis spectra of *n*-type and negatively charged nanocrystals. The changes in widths of these three Gaussians are constrained to be the same, and the shifts in the positions of the first and second exciton peaks are proportional to the ratio of their original positions with respect to the bulk band gap. That is, if the shift in the first exciton peak is ΔE , the

shift in the next exciton peak is constrained to be $\Delta E \times (E_2 - E_g)/(E_1 - E_g)$. E_1 and E_2 are the positions of the first and the second exciton peaks, respectively, of the nanocrystals before exposure to sodium biphenyl. E_g is the bulk band gap. The third peak does not follow the same proportional shift due to the fact that it is composed of several different transitions. There is also an additional term of the form $\text{constant} \times (E - E_g/2)^{2.5}$ to account for the visible tail.

(37) Norris, D. J.; Bawendi, M. G. *Phys. Rev. B* **1996**, 53, 16338.

(38) In this titration model, the partition function of CdSe nanocrystals with a 2-electron $1S_e$ state (0 eV), a 4-electron surface trap state (-0.02

eV), a 2-electron trap state (-0.16 eV), and a 2-electron trap state (-0.3 eV) is $Z = \sum_{j=0}^{10} \exp[-(E_j - j\mu)/kT]$, where E_j is the energy of the nanocrystals with j electrons. The oxidant, linearly introduced in time, has a partition function $Z_0 = 1 + \exp[-(E_0 - j\mu)/kT]$ between its reduced and oxidized form. Given an initial μ , the concentration of nanocrystals, the rate of introduction of the oxidant, the time evolution of μ , and the concentration of all the species are uniquely determined. The evolution of IR absorption, visible bleach and tail, and PL can then be reproduced as described in the text.